Performance Analysis on Wireless Power Transfer Wireless Sensor Network with Best AF Relay Selection over Nakagami-m Fading

Duy-Hung Ha[1], Dac-Binh Ha[2](✉), Van-An Vo[3], and Miroslav Voznak[1]

[1] Faculty of Electrical Engineering and Computer Science, VSB - Technical University of Ostrava, 17. lisltopadu 2172/15, 708 00 Ostrava, Czechia
haduyhung@tdtu.edu.vn, miroslav.voznak@vsb.cz

[2] Faculty of Electrical and Electronics Engineering, Duy Tan University, Danang, Vietnam
hadacbinh@duytan.edu.vn

[3] Faculty of Engineering Technology, Binh Duong Economics and Technology University, Binh Duong, Vietnam
vvan@ktkt.edu.vn

Abstract. In this paper, we present the performance analysis of energy harvesting amplify-and-forward (AF) relaying wireless sensor network with best relay selection scheme over Nakagami-m fading. Specifically, this considered network consists of one sink, multiple energy-constrained relays, and one destination sensor node. The best relay is chosen to amplify and forward the message to the destination after powered by the sink. In order to evaluate the performance, the closed-form expression of outage probability and throughput are derived by applying the discrete optimal power splitting ratio. Based on this expression, we investigate the behavior of this network according to the key parameters such as transmit power, number of relays, time switching ratio and the distance.

Keywords: Wireless sensor network · Wireless power · Relaying network · Amplify and forward · Time switching · Power splitting · Outage probability

1 Introduction

Nowadays, wireless sensor networks (WSNs) present extensive potential in human life, i.e., health monitoring, security and tactical surveillance, intrusion detection, manufacturing control, disaster management, weather monitoring, traceability, farming monitoring, and safety services. The next generation network (i.e., 5G), the platform of the Internet of Things (IoT), is developing

T. Q. Duong et al. (Eds.): INISCOM 2019, LNICST 293, pp. 193–204, 2019.
https://doi.org/10.1007/978-3-030-30149-1_16

to deploy in the near future. This drives the wide application of WSNs into real life. However, there are a number of challenges that WSNs faced when they are deployed widely, such as the limitations of the resource (i.e., processing ability, memory capacity, antenna, and battery capacity). The limited energy of sensor nodes degrade the coverage of WSN, reduce the processing ability of the sensor node and decrease the lifetime of the network.

A novel technology trend in energy harvesting that can solve the limited energy problem in WSNs is wireless power transfer, namely RF energy harvesting (EH). RF EH in WSNs (RF EH-WSNs) refers to the sensor nodes (SNs) harvest energy from RF energy sources (TV/radio broadcasts, mobile base stations, and handheld radios) and converting it into electrical energy for information transmission. Although the harvested energy from the above environmental sources is dependent on the presence of the energy sources and must consider their unstable natures, the RF energy harvesting approach may represent a practical trend for future energy-aware systems because of it's ready available in the form of transmitted energy and in small form factor implementations, and low cost [1–4]. The relaying and cooperative techniques are applied in the modern WSNs to improve the performance and extend the coverage area of wireless networks and reduce the energy consumption of SNs [5–10]. Naturally, the embedding EH into relaying WSNs or cooperative WSNs have attracted a lot of attention from the academia and industry in the recent decade [11–21]. There are two models of RF EH architecture: time switching (TS) and power splitting (PS). In the TS architecture, the SNs switch and use either the RF energy harvesting circuit or the information receiver circuit for the received RF signals, for example, a part of the time for energy harvesting and remain time for information receiving. Meanwhile, in the PS architecture, the received RF signals are split into two streams for the RF energy harvester circuit or information receiver circuit according to PS ratios. One problem introduced is how to find the optimal TS or PS ratio to enhance the performance of WSNs. In [13], the authors introduced the block-wise TS-based protocol for EH AF relaying network in which the relay can implement EH and information processing. By derivation of analytical expressions of the achievable throughput, the performance of this considered networks with two modes of continuous and discrete time EH at the relay was analyzed and evaluated. The PS-based protocol was applied at each relay of simultaneous wireless information and power transfer (SWIPT) multi-relay network to coordinate the received signal energy for information decoding and EH in [15]. By using the interior-point method, the solutions for the optimization problems of PS ratios at the relays were provided for both basic relay schemes, i.e., decode-and-forward (DF) and AF. In the work of [19], the authors proposed a hybrid TS-APS protocol for EH DF relay networks with the discrete-level battery of relays. The results of this work have shown that the proposed TS-APS scheme can achieve better effective transmission rate than the previous works. The authors in the work [20] analyzed the performance of an energy harvesting relay-aided cooperative network with proposed on-off relay-aided cooperative protocol. By the help of the Markov property of energy buffer status, the analytical closed-form expression of outage probability was derived for Nakagami-m fading channels. This paper concluded that this approach can improve the system outage performance when EH relays were employed and The studied results have also shown that the more relays the better system performance. A TSAPS-OBR protocol based on optimal capacity for energy harvesting AF relaying network was proposed in [21]. The optimal PS ratio was found to maximum the end-to-end SNR and the simulation results confirmed that the performance of this considered system is improved by applied this optimal value. However, they have not derived the expression of outage probability for performance analysis.

Motivate by the work of [21], in this paper we consider the AF multi-relay wireless sensor networks with RF energy harvesting over Nakagami-m fading channels. The main contributions of our paper are as follows.

1. Deriving the closed-form expressions of outage probability and throughput of this considered WSN in two cases: fixed and adaptive PS ratio.
2. Evaluating the performance of the considered system in different key system parameters, such as transmit SNR, EH time, relay location, and number of relays in two cases: fixed and adaptive PS ratio.

The remain of this paper is organized as follows. Section 2 presents the system and channel models. The closed-form expressions of outage probability and throughput are derived in Sect. 3. The numerical results and discussion are shown in Sect. 4. Finally, the conclusion of the paper is provided in Sect. 5.

Notation: P_0 is the transmit power of S; n represents additive Gaussian noise, i.e., $n \sim \mathcal{CN}(0, N_0)$; d_1 and d_2 are the distances of $S-R$ and $R-D$, respectively; θ is the path loss exponent, for simplicity, the path loss exponent is assumed the same for all relays; η $(0 \leq \eta \leq 1)$ is the energy conversion efficiency; $*$ is denoted as the best relay chosen according to TSAPS-ORS protocol [21].

2 System and Channel Models

The Fig. 1 depicts a RF EH AF wireless sensor network, where a sink node (S) communicates with destination sensor node (D) via the assistance of K energy-constrained relays R_k $(1 \leq k \leq K)$.

The operation scenario of this considered system is assumed as [21]. The dual-phase protocol for this considered system as follows:

(i) In the first phase, S broadcasts information/energy signal to the energy-constrained relays in the time of αT (α is the fraction of the block time, $0 \leq \alpha \leq 1$) based on TS scheme. The relays split the received signal into two parts with the splitting ratio ρ $(0 \leq \rho \leq 1)$ based on PS scheme: one part is for information signal and other parts for EH leaving for amplifying and retransmitting;
(ii) In the second phase of the remaining duration of $(1-\alpha)T$, the best relay selected among K relays amplifies the information part of RF signal received from S and retransmit to D by using the harvested energy in the first phase.

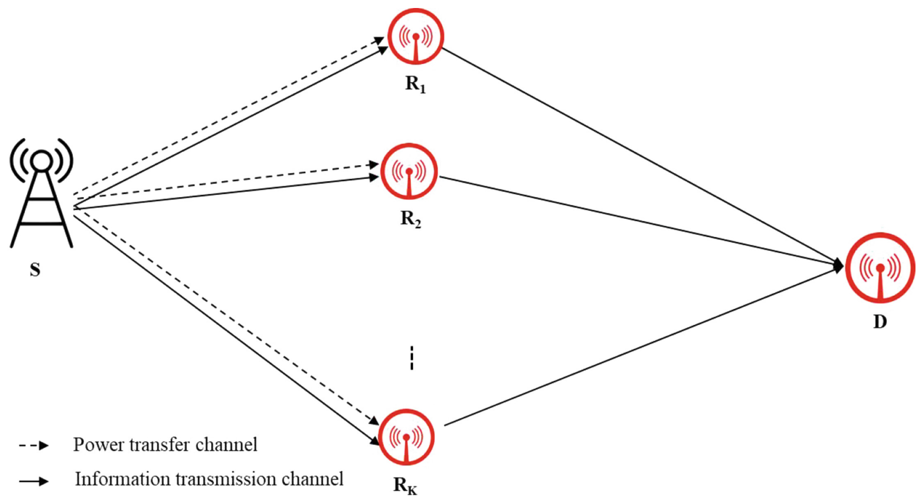

Fig. 1. System and channel models for EH AF WSNs

Note that, the PS ratio can be dynamically adjusted according to the variation of channel coefficient to maximum the end-to-end signal-to-noise ratio (SNR). Note that the optimal relay is selected among N AF relays based on the criteria of optimal system capacity. The relays can estimate the instantaneous channel gain based on the algorithm of channel estimation in request-to-send (RTS)/clear-to-send (CTS) transmission from the source and the destination [21].

According to [21], in high SNR region, the end-to-end SNR of this considered system is given by

$$\gamma_{e2e}^{*} \sim \frac{c\gamma_0\gamma_1^{*}\gamma_2^{*}(1-\rho^{*})\rho^{*}}{c(1-\rho^{*})\gamma_2^{*}+\rho^{*}}, \tag{1}$$

where $c = \dfrac{\eta\alpha}{1-\alpha}$, $\gamma_0 = \dfrac{P_0}{N_0}$, $\gamma_1^{*} = \dfrac{|h_1|^2}{d_1^{\theta}}$, $\gamma_2^{*} = \dfrac{|h_2|^2}{d_2^{\theta}}$.

In order to maximum γ_{e2e}^{*}, the optimal ρ^{*} was introduced in [21] as follows

$$\rho^{*} = \frac{\sqrt{c\gamma_2^{*}}}{\sqrt{c\gamma_2^{*}}+1}. \tag{2}$$

Due to the relay node can only split the received signal into two power parts based on a finite discrete set of PS ratios in practice, we design that ρ_i^{*} can only pick the value from the following set:

$$\rho_l \in \left\{\frac{1}{L}, \frac{2}{L}, \cdots, \frac{L-1}{L}\right\}, \tag{3}$$

where L is the number of PS ratio levels and $1 \leq l \leq L-1$. Note that, ρ_l^* cannot is selected as zero (no information part) or one (no energy part). According to (2) and (3), we assign $\rho_l^* = \dfrac{l}{L}$ when the channel gain of R - D link satisfies the following condition:

$$b_l = \frac{l^2}{(L-l)^2 c} < \gamma_2^* < b_{l+1} = \frac{(l+1)^2}{(L-l-1)^2 c}, \tag{4}$$

where $l \in \{1, 2, \cdots, L-1\}$.

Note that due to the links of S - R and R - D undergo the Nakagami-m fading, the cumulative distribution function (CDF) and probability density function (PDF) of random variable (RV) SNRs, i.e., γ_n, $n \in \{1,\, 2\}$ are respectively given by

$$F_{\gamma_n}(x) = 1 - e^{-\frac{m_n}{\lambda_n}x} \sum_{k=0}^{m_n-1} \frac{1}{k!} \left(\frac{m_n}{\lambda_n}x\right)^k, \tag{5}$$

$$f_{\gamma_n}(x) = \frac{x^{m_n-1}}{(m_n-1)!} \left(\frac{m_n}{\lambda_n}\right)^{m_n} e^{-\frac{m_n}{\lambda_n}x}, \tag{6}$$

where $\lambda_n = \mathbf{E}(\gamma_n)$, $m_n \geq 1/2$ is the fading severity factor, in which $m_n = 1$ corresponds to Rayleigh fading and $m_n = (V+1)^2/(2V+1)$ approximates Rician fading with parameter V.

3 Performance Analysis

This Section presents the derivation of the expression of outage probability and throughput of this considered WSN system.

System Outage Probability. In order to characterize the performance of a wireless communication system, the outage probability is used as an important performance metric. It is defined as the probability that the instantaneous capacity (C) falls below a predetermined rate threshold $R > 0$, which is expressed as

$$OP = \Pr(C < R). \tag{7}$$

In this considered system with TSAPS-ORS scheme [21], the overall outage probability can be obtained as

$$OP^* \overset{(a)}{=} (P_{out}^*)^K = \left[\Pr\left(C_{opt}^* < R\right)\right]^K = \left[\Pr(\gamma_{e2e}^* < 2^{\frac{2R}{1-\alpha}} - 1)\right]^K, \tag{8}$$

where C_{opt}^* is the optimal instantaneous capacity for best relay. Note that step (a) is obtained by assuming the channels are modeled as i.i.d over different relaying channels [19].

To analyze the performance of this system, we obtain the following theorems.

Theorem 1. Under Nakagami-m fading, the outage probability of overall system is obtained as

$$OP^{*} = \{1 - \sum_{l=1}^{L-1}\sum_{j=0}^{m_1-1}\sum_{i=0}^{j}\frac{e^{-\frac{m_1\gamma_{th}}{\lambda_1\rho_l\gamma_0}}}{i!(j-i)!(m_2-1)!c^i(1-\rho_l)^i\rho_l^{j-i}}\left(\frac{m_1\gamma_{th}}{\lambda_1\gamma_0}\right)^j\left(\frac{m_2}{\lambda_2}\right)^{m_2}$$
$$\times\sum_{p=0}^{\infty}\frac{(-1)^p a_1^p}{p!a_2^{m_2-i-p}}\left[\Gamma(m_2-i-p,a_2b_l)-\Gamma(m_2-i-p,a_2b_{l+1})\right]\}^K, \tag{9}$$

where $a_1 = \frac{m_1\gamma_{th}}{\lambda_1 c(1-\rho_l)\gamma_0}$, $a_2 = \frac{m_2}{\lambda_2}$.

Proof. See Appendix.

System Throughput. The second important and related performance metric is the throughput (τ) at the destination under the delay-limited transmission mode. This metric is found by evaluating the outage probability at a fixed source transmission rate $-$ R bps/Hz. Taking into account the fixed source transmission rate R bps/Hz, the effective communication time from the source node to the destination node in the total block time T is $\frac{(1-\alpha)T}{2}$. We obtain the following theorem.

Theorem 2. Under Nakagami-m fading, the overall throughput of this considered system is written as

$$\tau = \frac{1}{2}(1-\alpha)R\Big\{1-\Big\{1-\sum_{l=1}^{L-1}\sum_{j=0}^{m_1-1}\sum_{i=0}^{j}\frac{e^{-\frac{m_1\gamma_{th}}{\lambda_1\rho_l\gamma_0}}}{i!(j-i)!(m_2-1)!c^i(1-\rho_l)^i\rho_l^{j-i}}\left(\frac{m_1\gamma_{th}}{\lambda_1\gamma_0}\right)^j$$
$$\times\left(\frac{m_2}{\lambda_2}\right)^{m_2}\sum_{p=0}^{\infty}\frac{(-1)^p a_1^p}{p!a_2^{m_2-i-p}}\left[\Gamma(m_2-i-p,a_2b_l)-\Gamma(m_2-i-p,a_2b_{l+1})\right]\Big\}^K\Big\}. \tag{10}$$

Proof. According to the definition of throughput [14], we have

$$\tau = (1-OP^{*})\,R\frac{(1-\alpha)T/2}{T} = \frac{1}{2}(1-\alpha)R\,(1-OP^{*})\,. \tag{11}$$

Substituting (9) into (11), we obtained the throughput of this considered system as (10). This is the end of our proof.

4 Numerical Results and Discussion

In this section, we provide the simulation and analysis results in terms of OP^{*} and τ to reveal the impact of key system parameters on system performance, such as average transmit SNR (γ_0), number of relays (N), TS ratio (α), EH efficiency (η), relay location (d_1) and fading severity factor (m).

4.1 Impact of Average Transmit SNR and Number of Relays

The impact of average transmit SNR γ_0 and the number of relays K on system performance are shown in Figs. 2 and 3. According to these figures, the performance gets better with increasing γ_0 and K. This is because the higher transmit power the better signal and the more energy harvested, leading to the higher power to amplify the retransmit signal in the second phase. However, when γ_0

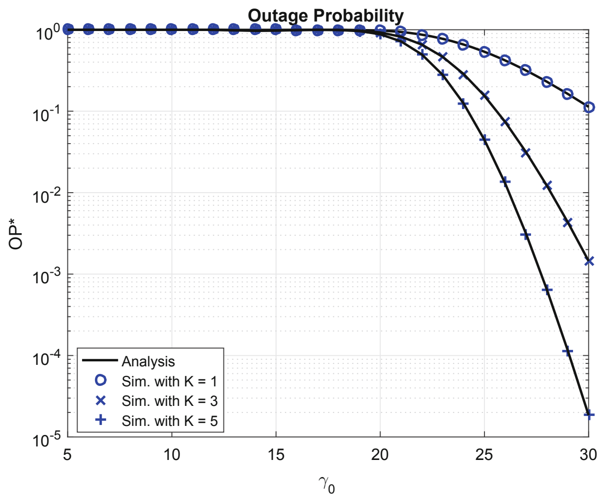

Fig. 2. OP^* vs. average transmit SNR γ_0 with $d_1 = d_2 = 1$, $m_1 = 2$, $m_2 = 25$, $R = 1\,\text{bps/Hz}$, $\theta = 2$, $\alpha = 0.7$, $\eta = 1$, $L = 20$.

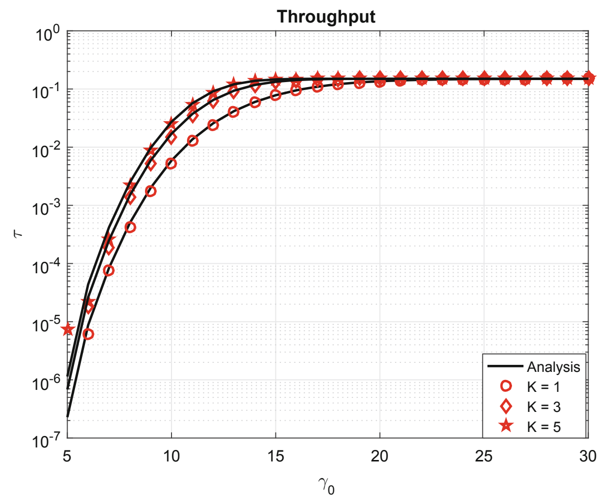

Fig. 3. τ vs. average transmit SNR γ_0 with $d_1 = d_2 = 1$, $m_1 = 2$, $m_2 = 25$, $R = 1\,\text{bps/Hz}$, $\theta = 2$, $\alpha = 0.7$, $\eta = 1$, $L = 20$.

is large enough, $OP^* \rightarrow 0$ and $\tau \rightarrow \frac{(1-\alpha)R}{2}$. From these figures, we can also understand that increasing the number of relays can improve the performance of this system because we have more choices to select the best relay to forward the information to the destination sensor node.

4.2 Impact of Energy Harvesting Time and Energy Harvesting Efficiency

Figures 4 and 5 plot the outage probability and throughput of this considered system versus α and η, respectively. It is seen from Figs. 4 and 5 that when α

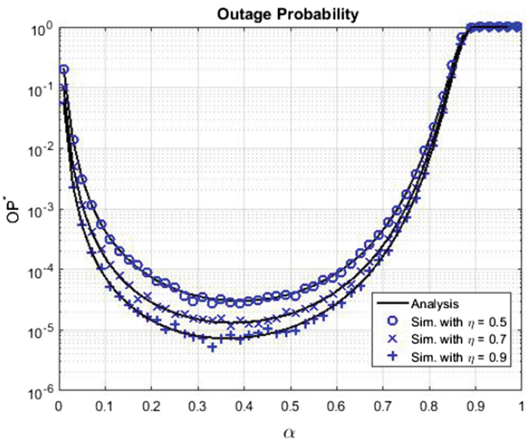

Fig. 4. OP^* vs. α and η with $\gamma_0 = 20\,\text{dB}$, $d_1 = d_2 = 1$, $m_1 = 2$, $m_2 = 15$, $R = 1\,\text{bps/Hz}$, $\theta = 2$, $L = 20$.

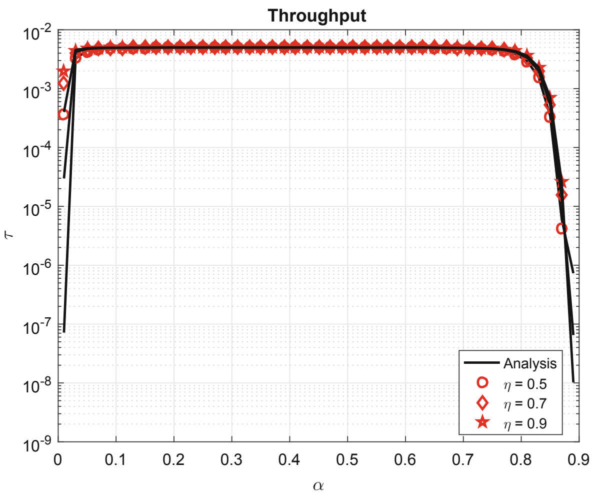

Fig. 5. τ vs. α and η with $\gamma_0 = 20\,\text{dB}$, $d_1 = d_2 = 1$, $m_1 = 2$, $m_2 = 15$, $R = 1\,\text{bps/Hz}$, $\theta = 2$, $L = 20$.

grow up, OP^* decreases, τ scales up and the performance is upgraded. This is explained that due to more time spent on energy harvesting as α grows leads to higher transmission power, hence better performance results. However, when α continues to increase, OP^* gets larger, τ scales down and the performance is degraded. That is because the information time is reduced, which leads to the increasing of real data rate. Overall, there is an optimal value of α that can minimize OP^*. This is clearly seen by the single bottom of the OP^* curve plotted in Fig. 4 as a function of α.

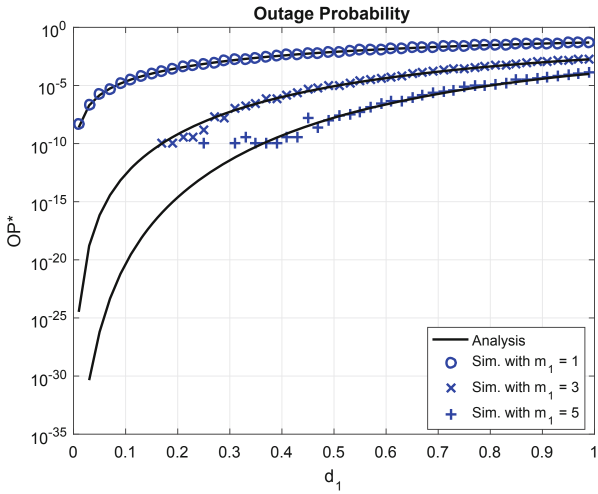

Fig. 6. OP^* vs. d_1 and m_1 with $\gamma_0 = 20$ dB, $d_2 = 2 - d_1$, $m_2 = 25$, $R = 1$ bps/Hz, $\theta = 2$, $\alpha = 0.7$, $\eta = 1$, $L = 20$.

4.3 Impact of Relay Location and Fading Severity Parameters

The impact of relay location (d_1) and fading severity parameters (m_1) on outage probability and throughput are illustrated in Figs. 6 and 7, respectively. In these two figures, increasing d_1 makes OP^* and τ worse. This is because of the higher values of d_1^{θ} lead to the smaller values of energy collected as well as poorer received signal strength at the relay nodes. Similarly, we can understand that OP^* decreases and τ increases with increasing m_1. This is because the channel qualities are better with larger fading severity parameters.

In general, from above figures we can see that the superior match between analytical and simulation results occurs in the high average transmit SNR or in large P_0 region. For a more clear explanation, when γ_0 holds low values, the analytical and simulation results do not match well because we use the approximated expression of the end-to-end SNR at the destination node as (1) [21] and using finite terms of (1.211-1) in [22].

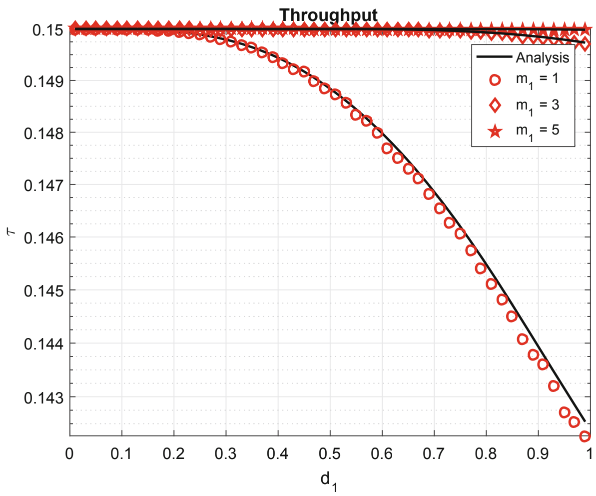

Fig. 7. τ vs. d_1 and m_1 with $\gamma_0 = 20\,\text{dB}$, $d_2 = 2 - d_1$, $m_2 = 25$, $R = 1\,\text{bps/Hz}$, $\theta = 2$, $\alpha = 0.7$, $\eta = 1$, $L = 20$.

5 Conclusion

In this paper, the closed-form expressions of outage probability and throughput have been derived. The simulation and analysis results have been presented to verify our derivations. Once again, these results have shown that the performance of this system can be improved by applying the TSAPS-ORS protocol.

Appendix

Here, we derive the expression of P^*_{out} as (12) on the top of next page. Substituting (12) into (8), we obtain the closed-form expression of outage probability for this system.

$$
\begin{aligned}
P^*_{out} &= \Pr(\gamma^*_{e2e} < 2^{\frac{2R}{1-\alpha}} - 1) \\
&= 1 - \sum_{l=1}^{L-1} \Pr\left(\frac{c\gamma_0\gamma_1\gamma_2(1-\rho_l)\rho_l}{c(1-\rho_l)\gamma_2 + \rho_l} > \gamma_{th}, b_l \le \gamma_2 < b_{l+1}\right) \\
&= 1 - \sum_{l=1}^{L-1} \int_{b_l}^{b_{l+1}} \left[1 - F_{\gamma_1}\left(\frac{c(1-\rho_l)\gamma_{th}x + \rho_l\gamma_{th}}{c(1-\rho_l)\rho_l\gamma_0 x}\right)\right] f_{\gamma_2}(x)dx \\
&= 1 - \sum_{l=1}^{L-1}\sum_{j=0}^{m_1-1}\sum_{i=0}^{j} \frac{e^{-\frac{m_1\gamma_{th}}{\lambda_1\rho_l\gamma_0}}}{i!(j-i)!(m_2-1)!c^i(1-\rho_l)^i\rho_l^{j-i}} \left(\frac{m_1\gamma_{th}}{\lambda_1\gamma_0}\right)^j \left(\frac{m_2}{\lambda_2}\right)^{m_2} \\
&\times \int_{b_l}^{b_{l+1}} x^{m_2-i-1} e^{-\frac{m_1\gamma_{th}}{\lambda_1 c(1-\rho_l)\gamma_0 x} - \frac{m_2 x}{\lambda_2}} dx
\end{aligned}
$$

$$
\begin{aligned}
&= 1 - \sum_{l=1}^{L-1}\sum_{j=0}^{m_1-1}\sum_{i=0}^{j} \frac{e^{-\frac{m_1\gamma_{th}}{\lambda_1\rho_l\gamma_0}}}{i!(j-i)!(m_2-1)!c^i(1-\rho_l)^i\rho_l^{j-i}} \left(\frac{m_1\gamma_{th}}{\lambda_1\gamma_0}\right)^j \left(\frac{m_2}{\lambda_2}\right)^{m_2} \\
&\times \left[\int_{b_l}^{\infty} x^{m_2-i-1} e^{-\frac{m_1\gamma_{th}}{\lambda_1 c(1-\rho_l)\gamma_0 x}-\frac{m_2 x}{\lambda_2}}dx - \int_{b_{l+1}}^{\infty} x^{m_2-i-1} e^{-\frac{m_1\gamma_{th}}{\lambda_1 c(1-\rho_l)\gamma_0 x}-\frac{m_2 x}{\lambda_2}}dx\right] \\
&\overset{(b)}{=} 1 - \sum_{l=1}^{L-1}\sum_{j=0}^{m_1-1}\sum_{i=0}^{j} \frac{e^{-\frac{m_1\gamma_{th}}{\lambda_1\rho_l\gamma_0}}}{i!(j-i)!(m_2-1)!c^i(1-\rho_l)^i\rho_l^{j-i}} \left(\frac{m_1\gamma_{th}}{\lambda_1\gamma_0}\right)^j \left(\frac{m_2}{\lambda_2}\right)^{m_2} \\
&\times \left[\sum_{p=0}^{\infty}\frac{(-1)^p a_1^p}{p!}\int_{b_l}^{\infty} x^{m_2-i-p-1}e^{-a_2x}dx - \sum_{q=0}^{\infty}\frac{(-1)^q a_1^q}{q!}\int_{b_{l+1}}^{\infty} x^{m_2-i-q-1}e^{-a_2x}dx\right] \\
&\overset{(c)}{=} 1 - \sum_{l=1}^{L-1}\sum_{j=0}^{m_1-1}\sum_{i=0}^{j} \frac{e^{-\frac{m_1\gamma_{th}}{\lambda_1\rho_l\gamma_0}}}{i!(j-i)!(m_2-1)!c^i(1-\rho_l)^i\rho_l^{j-i}} \left(\frac{m_1\gamma_{th}}{\lambda_1\gamma_0}\right)^j \left(\frac{m_2}{\lambda_2}\right)^{m_2} \\
&\times \left[\sum_{p=0}^{\infty}\frac{(-1)^p a_1^p}{p! a_2^{m_2-i-p}}\Gamma(m_2-i-p, a_2 b_l) - \sum_{q=0}^{\infty}\frac{(-1)^q a_1^q}{q! a_2^{m_2-i-q}}\Gamma(m_2-i-q, a_2 b_{l+1})\right], \qquad (12)
\end{aligned}
$$

where $\gamma_{th} = 2^{\frac{2R}{(1-\alpha)}} - 1$. Note that step (b) and (c) are obtained by the help of (1.211-1) and (3.381-3), respectively, in [22].

This concludes our proof.

References

1. Chen, X., Zhang, Z., Chen, H.H., Zhang, H.: Enhancing wireless information and power transfer by exploiting multi-antenna techniques. IEEE Commun. Mag. **53**(4), 133–141 (2015)
2. Ha, D.B., Tran, D.D., Truong, T.V., Vo, N.V.: Physical layer secrecy performance of energy harvesting networks with power transfer station selection. In: IEEE International Conference on Communications and Electronics (ICCE), pp. 451–456 (2016)
3. Vo, V.N., Nguyen, T.G., So-In, C., Ha, D.B.: Secrecy performance analysis of energy harvesting wireless sensor networks with a friendly jammer. IEEE Access (2017)
4. Xu, K., Shen, Z., Wang, Y., Xia, X.: Beam-domain hybrid time-switching and power splitting SWIPT in full-duplex massive MIMO system. EURASIP J. Wirel. Commun. Netw., 1–21 (2018)
5. Suraweera, H.A., Karagiannidis, G.K., Smith, P.J.: Performance analysis of the dual-hop asymmetric fading channel. IEEE Trans. Wirel. Commun. **8**(6), 2783–2788 (2009)
6. Gurung, A.K., AI-Qahtani, F.S., Hussain, Z.M., Alnuweiri, H.: Performance analysis of amplify-forward relay in mixed Nakagami-m and Rician fading channels. In: The 2010 International Conference on Advanced Technologies for Communications, Ho Chi Minh City, Vietnam, 20–22 October 2010, pp. 321–326 (2010)

7. Haghighat, J., Eslami, M., Hamouda, W.: Relay pre-selection for reducing CSI transmission in wireless sensor networks. IEEE Commun. Lett. **20**(9), 1828–1831 (2016)
8. Mousavi, S.H., Haghighat, J., Hamouda, W., Dastbasteh, R.: Analysis of a subset selection scheme for wireless sensor networks in timevarying fading channels. IEEE Trans. Signal Process. **64**(9), 2193–2208 (2016)
9. Kim, J.B., Song, M.S., Lee, I.H.: Achievable rate of best relay selection for non-orthogonal multiple access-based cooperative relaying systems. In: International Conference on Information and Communication Technology Convergence (ICTC), Jeju, South Korea, pp. 960–962. IEEE (2016)
10. Gendia, A.H., Elsabrouty, M., Emran, A.A.: Cooperative multi-relay non-orthogonal multiple access for downlink transmission in 5G communication systems. In: 2017 Wireless Days, Porto, Portugal. IEEE (2017)
11. Luo, Y., Zhang, J., Letaief, K.B.: Relay selection for energy harvesting cooperative communication systems. In: IEEE Global Communications Conference (GLOBECOM), pp. 2514–2519 (2013)
12. Ishibashi, K.: Dynamic harvest-and-forward: new cooperative diversity with RF energy harvesting. In: 2014 Sixth International Conference on Wireless Communications and Signal Processing (WCSP), 23–25 October 2014, pp. 1–5 (2014)
13. Nasir, A.A., Zhou, X., Durrani, S., Kennedy, R.A.: Block-wise time-switching energy harvesting protocol for wireless-powered AF relays. In: 2015 IEEE International Conference on Communications (ICC), 8–12 June 2015, pp. 80–85 (2015)
14. Ha, D.B., Tran, D.D., Tran-Ha, V., Hong, E.K.: Performance of amplify-and-forward relaying with wireless power transfer over dissimilar channels. Elektronika ir Elektrotechnika J. **21**(5), 90–95 (2015)
15. Liu, Y.: Wireless information and power transfer for multi-relay assisted cooperative communication. IEEE Commun. Lett. **20**(4), 784–787 (2016)
16. Nguyen, H.S., Do, D.T., Nguyen, T.S., Voznak, M.: Exploiting hybrid time switching-based and power splitting-based relaying protocol in wireless powered communication networks with outdated channel state information. J. Control Meas. Electron. Comput. Commun. **58**(1), 111–118 (2017)
17. Ha, D.B., Nguyen, Q.S.: Outage performance of energy harvesting DF relaying NOMA networks. Mobile Netw. Appl. (2017)
18. Cvetkovic, A., Blagojevic, V., Ivanis, P.: Performance analysis of nonlinear energy-harvesting DF relay system in interference-limited Nakagami-m fading environment. ETRI J. **39**(6), 803–812 (2017)
19. Singh, V., Ochiai, H.: A efficient time switching protocol with adaptive power splitting for wireless energy harvesting relay networks. In: IEEE 85th Vehicular Technology Conference (VTC Spring) (2017)
20. Zhong, S., Huang, H., Li, R.: Performance analysis of energy-harvesting-aware multi-relay networks in Nakagami-m fading. EURASIP J. Wirel. Commun. Netw. **2018**, 63 (2018)
21. Ha, D.H., Ha, D.B., Zdralek, J., Voznak, M.: A new protocol based on optimal capacity for energy harvesting amplify-and-forward relaying networks. In: 5th NAFOSTED Conference on Information and Computer Science (NICS), HCMC, Vietnam (2018)
22. Gradshteyn, I., Ryzhik, I.: Table of Integrals, Series, and Products. Elsevier Academic Press, Cambridge (2007)